

Neutron Spectroscopy as a Probe of Macromolecular Structure and Dynamics under Extreme Spatial Confinement

This content has been downloaded from IOPscience. Please scroll down to see the full text.

2014 J. Phys.: Conf. Ser. 549 012009

(<http://iopscience.iop.org/1742-6596/549/1/012009>)

View [the table of contents for this issue](#), or go to the [journal homepage](#) for more

Download details:

IP Address: 161.111.180.191

This content was downloaded on 20/09/2016 at 12:05

Please note that [terms and conditions apply](#).

You may also be interested in:

[The use of direct geometry spectrometers in molecular spectroscopy](#)

Stewart F Parker, Anibal J Ramirez-Cuesta, Peter W Albers et al.

[Recent and future developments on TOSCA at ISIS](#)

Stewart F Parker, Felix Fernandez-Alonso, Anibal J Ramirez-Cuesta et al.

[LAGRANGE - the new neutron vibrational spectrometer at the ILL](#)

Mónica Jiménez-Ruiz, Alexander Ivanov and Stephane Fuard

[Sample environment issues relevant to the acquisition of inelastic neutron scattering measurements of heterogeneous catalyst samples](#)

R Warringham, D Bellaire, S F Parker et al.

[Confined dynamics in poly\(ethylene terephthalate\): a coherent and incoherent neutron scattering study](#)

Alejandro Sanz, Aurora Nogales, Inés Puente-Orench et al.

[IN1-LAGRANGE – the new ILL instrument to explore vibration dynamics of complex materials](#)

Alexandre Ivanov, Mónica Jimenéz-Ruiz and Jiri Kulda

Neutron Spectroscopy as a Probe of Macromolecular Structure and Dynamics under Extreme Spatial Confinement

F Barroso-Bujans,^{1,*} F Fernandez-Alonso^{2,3} and J Colmenero^{1,4,5}

¹Centro de Física de Materiales (CSIC-UPV/EHU)-Material Physics Center (MPC), Paseo Manuel Lardizábal 5, 20018 San Sebastian, Spain

²ISIS Facility, Rutherford Appleton Laboratory, Chilton, Didcot, Oxfordshire OX11 0QX, United Kingdom

³Department of Physics and Astronomy, University College London, Gower Street, London, WC1E 6BT, United Kingdom.

⁴Departamento de Física de Materiales, Universidad del País Vasco (UPV/EHU) Aptdo 1072, 20080 San Sebastian, Spain

⁵Donostia International Physics Center, Paseo Manuel Lardizábal 4, 20018 San Sebastian, Spain

E-mail: fbarroso@ehu.es

Abstract. We illustrate the use of high-resolution neutron spectroscopy to explore the extreme spatial confinement of soft matter in nanostructured materials. Two well-defined limits are considered, involving either intercalation or interfacial adsorption of the ubiquitous polymer poly(ethylene oxide) in graphite-oxide-based hosts. Vibrational modes associated with the confined macromolecular phase undergo dramatic changes over a broad range of energy transfers, from those associated with intermolecular modes in the Terahertz frequency range (1 THz = 33 cm⁻¹), to those characteristic of strong chemical bonds above 2000 cm⁻¹. We also consider the effects of polymer chain size and chemical composition of the host material. Variation of the degree of oxidation and exfoliation of graphite oxide leads to two distinct cases, namely: (i) subnanometer two-dimensional confinement; and (ii) surface immobilization. Case (i) is characterised by significant changes to conformational and collective vibrational modes of the polymer as a consequence of a preferentially planar trans-trans-trans chain conformation, whereas case (ii) leads to a substantial increase in the population of gauche conformers. Macroscopically, case (i) translates into the complete suppression of crystallization and glassy behaviour. In contrast, case (ii) exhibits well-defined glass and melting transitions associated with the confined phase, yet at significantly lower temperatures than those of the bulk.

1. Introduction

Optical spectroscopy has been used extensively to characterise polymeric and macromolecular materials [1]. Traditionally, Fourier-transform Infrared (FTIR) and Raman spectroscopy have been the most versatile methods to identify specific structural features related to polymer conformation in the solid and molten phases. The ubiquitous polymer poly(ethylene oxide), hereafter PEO, is a good case in point, as the solid phase is characterised by a distinct helical



structure which is only retained partially in the liquid or under conditions of strong spatial confinement [2, 3, 4].

Notwithstanding the above, optical spectroscopic techniques do fail in some important cases of increasing scientific and technological interest. Such is the case of macromolecular intercalation or adsorption in layered and nanostructured host media, particularly when the latter is characterised by a strong optical response in the spectral range of interest. Graphite-based substrates fall into this problematic class of materials owing to their strong absorption in the infrared [5] or electronic (resonant) enhancement effects in the visible region of the electromagnetic spectrum [6, 7]. Owing to the strong neutron-proton incoherent cross section, inelastic neutron scattering (INS) can circumvent these difficulties quite elegantly in the microscopic characterisation of confined hydrogenous matter. We have recently demonstrated how broadband, high-resolution INS, as that afforded by the TOSCA spectrometer at the ISIS Facility (United Kingdom) [8], constitutes an exquisite characterisation tool to study soft hydrogenous matter confined in graphite-oxide (GO) materials [9, 10, 11].

In this contribution to the Proceedings of the VI Meeting of the Spanish Neutron Scattering Association, we highlight the merits and strengths of INS as a tool to characterise molecular and macromolecular structure and dynamics under extreme spatial confinement. To this end, we compare INS data obtained for PEO chains of increasing length, from a single monomeric unit [i.e., ethylene glycol (EG)] to several thousand repetitive ethylene-oxide units. Furthermore, by varying the degree of GO oxidation and exfoliation, we also explore distinct regimes of spatial confinement, from subnanometer two-dimensional confinement to surface immobilization onto graphene (G) sheets. We close by outlining both the basic instrumental prerequisites that have enabled these studies as well as some ways forward.

2. Experimental

2.1. *Synthesis of graphite-oxide-based materials and intercalation compounds*

GOs were produced by oxidation of natural graphite using a modified Brodie method [12]. Varying degrees of GO oxidation were obtained by changing the reaction time and temperature [9, 13]. Specimen G was obtained by placing GO on a glass boat and inserting it in a quartz tube under an argon flux. This tube was then inserted into a tube furnace preheated to 1000 °C. After 1 min, the tube was removed and cooled down to room temperature. Pentaethylene glycol (5PEO) was purchased from Fluka, whereas EG and PEO [HO(CH₂CH₂O)_nH] with chain lengths $n = 13, 104, 795, \text{ and } 2135$ were supplied by Aldrich. Hereafter, we will use the term “nPEO” to identify a PEO chain of length “n.” Intercalation of EG and 5PEO was performed by direct mixing with GO in the absence of solvent, whereas intercalation of 13PEO and 2135PEO was carried out in aqueous solution by stirring a total of 0.5 g PEO previously dissolved in 20 mL water with 0.5 g GO over a period of 15 days. A similar procedure was followed to absorb 2135PEO onto the G specimen. Any EG and PEO excess was removed by filtration and thorough aqueous washings. The resulting EG/GO, nPEO/GO ($n=5, 13 \text{ and } 2135$) and 2135PEO/G specimens were then dried at 80°C for 24 h in a vacuum oven ($P < 0.1 \text{ mbar}$). The amount of EG(nPEO) in EG(nPEO)/GO and nPEO/G was calculated from thermogravimetric sample-residue analysis as described previously in Refs. [10, 14]. Additional compositional and structural information can be found in Ref. [13].

2.2. *Characterisation*

INS experiments were performed on the TOSCA spectrometer [8] located at the ISIS Facility, Rutherford Appleton Laboratory, United Kingdom. Neutron time-of-flight data were collected in both back- and forward-scattering geometries, and then added together to obtain a hydrogen-projected vibrational density of states (VDOS). Typical run times varied between 2 and 8 h depending on the hydrogen content of the sample. All samples were contained in flat aluminium

cells of thickness 1-4 mm and cooled to temperatures below 30 K. Based on the thermal behaviour of EG and nPEO observed by differential scanning calorimetry (DSC), EG and nPEO with $n \geq 13$ cannot be obtained in an amorphous state, whereas the quenching of molten 5PEO in liquid nitrogen can prevent crystallisation. Amorphous 5PEO was then produced by direct immersion (quenching) into the TOSCA cryostat ($T < 30\text{K}$). Crash cooling to cryogenic temperatures ($T < 100\text{K}$) was optimised by placing the samples at the bottom of the cryostat and exposing them directly to a stream of liquid helium. To prepare a crystalline sample of 5PEO, the specimen was first crystallised in a freezer held at 240K , followed by immersion in the low-temperature cryostat. INS data of GO, G, EG, and nPEO were normalized to sample mass and those of EG(nPEO)/GO and 2135PEO/G were normalized to the amount of EG(nPEO) content.

3. Results and Discussion

3.1. Molecular-size effects

Both EG and nPEO intercalate into the GO interlayer space giving rise to a single molecular layer of thickness $3.0\text{-}3.4 \text{ \AA}$. Their concentration in the intercalate amounts to $22 \pm 2 \text{ wt}\%$ of the total EG(nPEO)/GO mass. Both the interlayer spacing and the amount of EG and nPEO do not depend strongly on intercalate chain length, a strong indication that the oligomer and polymer chains are forced to adopt a planar conformation in a monolayer arrangement, i.e., well-defined and extreme two-dimensional (2D) confinement. Moreover, neither EG nor nPEO can crystallize in the intercalate and their corresponding glass transitions are not present in the calorimetric data. Previous dielectric-spectroscopy studies to probe the α -relaxation process (associated with the glass transition) and other processes related to molecular mobility below the glass transition have also shown the suppression of α -relaxation phenomena as well as a slowdown of β -relaxation modes for 2135PEO [11]. These results were rationalized in terms of a complete suppression of cooperativity among polymer chains and restricted chain motions induced by strong (hydrogen-bonding) PEO-GO interactions. On the basis of the above experimental results, the cartoon in Figure 1 provides a schematic representation of the EG/GO and 5PEO/GO materials of relevance to the present study.

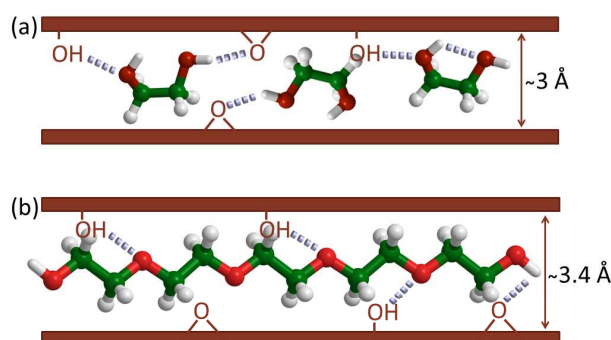


Figure 1. Sketch of (a) EG/GO and (b) 5PEO/GO intercalates. Dashed lines show the intermolecular hydrogen bonds between the EG(5PEO) intercalate and the GO host.

Figure 2 shows the attenuated-total-reflectance Fourier-transform infrared (ATR-FTIR) spectrum of GO, as well as those of bulk and confined PEO with the longest chain length of the series (2135PEO). As observed, FTIR spectral features associated with confined PEO are severely affected by the presence of a highly absorbing GO matrix, making it practically

impossible to extract quantitative information on changes to the vibrational spectrum of the polymer upon intercalation. The most significant changes in these ATR-FTIR data take place in the OH stretch region at ca. 3250 cm^{-1} , associated with the presence of hydroxyl (OH) groups in the GO substrate. The red shift observed in going from pristine GO to 2135PEO/GO indicates the formation of hydrogen bonds between OH groups in GO and PEO ether groups, and are associated with an overall weakening of O-H bonds [15]. This assignment is also supported by a red shift of the C-O-C stretching vibration band centred at 1103 cm^{-1} in bulk PEO. The FTIR data thus confirms the presence of specific intermolecular interactions between PEO and GO, yet it provides no direct information about the confined polymer phase.

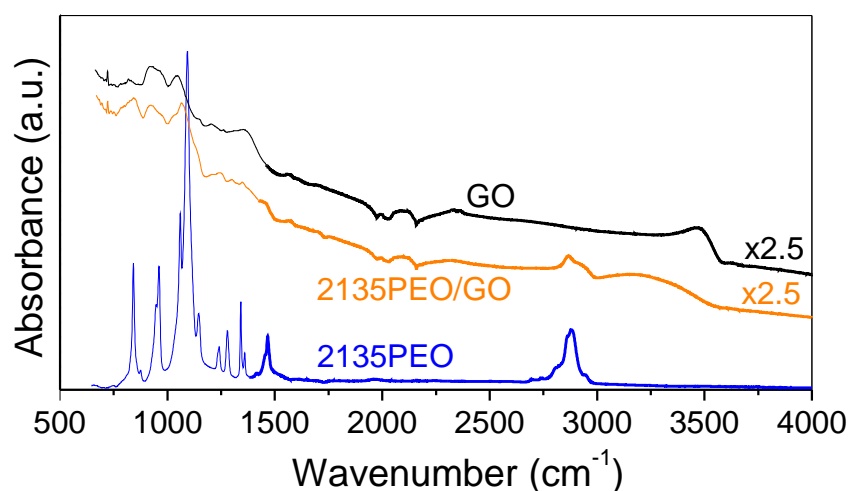


Figure 2. Room-temperature ATR-FTIR spectra of GO, bulk 2135PEO, and 2135PEO/GO. For ease of comparison, the overall intensities of the spectra corresponding to GO and 2135PEO/GO have been multiplied by a factor of 2.5.

To gain further insight into the macromolecular structure of confined EG and nPEO, INS measurements on EG/GO, nPEO/GO, and their corresponding pristine materials were performed on the TOSCA spectrometer at 30 K. One of the primary advantages of INS spectroscopy is that there are no hard selection rules and mode intensities can be directly related to the underlying VDOS. Therefore, spectral assignments can be performed on the basis of our current understanding of the vibrational spectrum of the bulk polymer obtained from optical spectroscopy [16, 17, 18] and computer simulation [19]. Another advantage of INS spectroscopy lies in its high sensitivity to vibrational modes involving hydrogen, thereby greatly simplifying spectral assignment when the host matrix is non hydrogenous. A detailed assignment of these bands has been reported in Refs. [10, 11]. Last but not least, INS spectroscopy allows access to very low energy transfers below $\sim 200\text{ cm}^{-1}$, difficult to access with conventional infrared and Raman techniques.

INS spectra for bulk and confined GO, EG, and nPEO ($n=5,13$, and 2135) over the energy-transfer range $24\text{-}4000\text{ cm}^{-1}$ are shown in Figure 3. The GO spectrum exhibits a very weak and featureless INS response, which enables a clear identification of EG(nPEO) bands in the EG(nPEO)/GO samples. At higher energy transfers (shaded region I in Figure 3), the INS spectra is dominated by a broad band associated with C-H stretch vibrations centred at $2930\text{-}2960\text{ cm}^{-1}$. The integrated intensity of this high-energy feature corresponding to C-H stretch modes serves to validate the amount of EG(nPEO) in the sample (ca. 22 wt%), as detailed previously in reference [11] for the case of the 2135PEO/GO intercalate. Moreover, we find that this particular spectral feature does not undergo any changes in intensity or line shape

upon confinement and can, therefore, be used as a reliable estimator of the total concentration of hydrogen in a given sample. On the basis of these observations, intensity changes at lower energy transfers can then be linked to changes in the vibrational dynamics of the intercalate upon confinement.

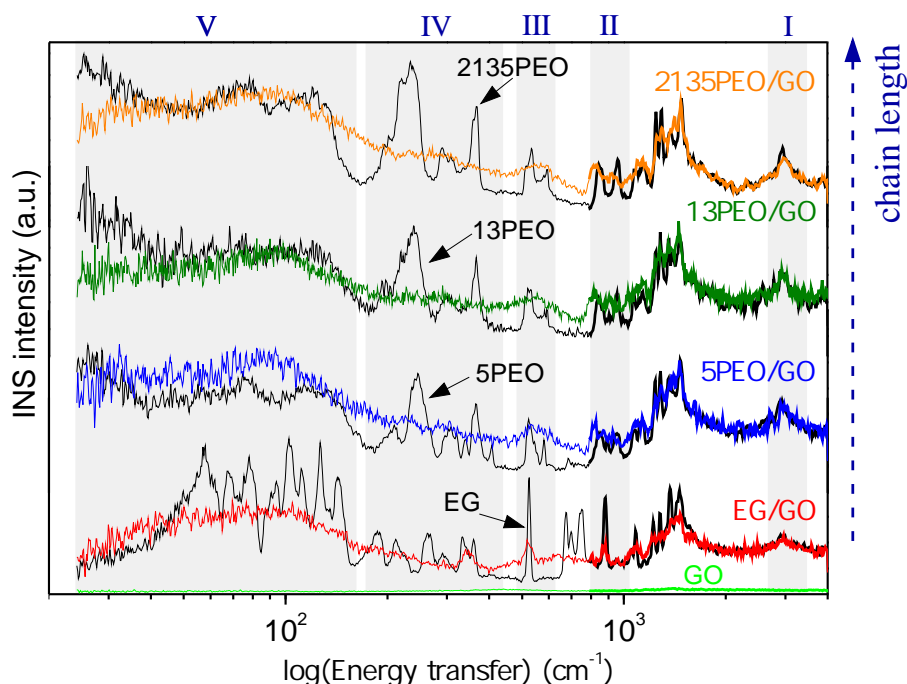


Figure 3. Mass-normalised INS spectra of GO, EG, and PEO ($n = 5-2135$) in the bulk and under confinement in GO (EG/GO and n PEO/GO). For an explanation of each shaded region in the spectra, see the main text.

The most significant differences between bulk and confined EG(n PEO) are observed at energy transfers below 1000 cm^{-1} (shaded regions II-V in Figure 3). INS spectral bands either disappear, shift, or broaden in confined EG(n PEO) compared to the bulk. We can rationalize these results in terms of restricted EG(n PEO) motions within the 2D GO interlayer. These spectral regions are discussed in more detail below.

Region II: CH_2 rocking modes [$r(\text{CH}_2)$] in the spectral range $800-1000 \text{ cm}^{-1}$ are particularly sensitive to macromolecular conformation for n PEO (i.e., *trans* and *gauche* conformers). These spectral features are also quite sensitive to temperature, dilution, metal coordination, and geometric constraints [20, 16, 21, 17, 18]. The band at 846 cm^{-1} corresponds to *trans-gauche-trans* (*tgt*) conformations of CCOC, OCCO, and COCC groups in crystalline n PEO. This band moves down to 831 cm^{-1} in the amorphous phase for the quenchable 5PEO bulk material [10], indicating a sensible increase in the population of *trans* conformers. In intercalated n PEO, this band moves further down to 814 cm^{-1} as a result of the predominance of *trans-trans-trans* (*ttt*) geometries [18, 20]. This assignment is further corroborated by the red shift and intensity suppression of the peak at 953 cm^{-1} and 943 cm^{-1} , corresponding to *tgt* conformations in the crystal and in the amorphous phase, respectively. Table 1 summarizes the position of $r(\text{CH}_2)$ bands for crystalline, amorphous, and confined 5PEO.

Region III: this spectral range ($480-600 \text{ cm}^{-1}$) provides information on the molecular conformation of EG. On the basis of infrared and Raman data for liquid and solid EG [22, 23], as well as for EG confined in silica-glass pores of radii 3-7 nm [24], the INS band at 523

cm^{-1} corresponds to the asymmetric CCO bending mode of the OCCO skeleton of the gauche conformer for crystalline EG [10]. The presence of a broad INS peak at 521 cm^{-1} , as well as the absence of a peak at 482 cm^{-1} (trans conformers [22]) for EG/GO indicates that EG adopts a disordered gauche conformation upon confinement.

Table 1. INS bands corresponding to CH_2 rocking vibrations in crystalline, amorphous, and confined 5PEO.

phase	Band 1	Band 2	conformation
crystalline	953	846	<i>tgt</i>
amorphous	943	831	intermediate
confined	928	816	<i>ttt</i>

Region IV: changes in the longitudinal-acoustic-mode (LAM) region ($150\text{-}400 \text{ cm}^{-1}$) [19] provide more evident signatures of changes to macromolecular conformation. These bands correspond to complex modes associated with collective vibrations along the polymer chain. From the INS data, the absence of peaks in the LAM region for all confined nPEO chains as compared to their bulk counterparts is quite apparent. Such a result is largely insensitive to molecular size and suggests the emergence of a new set of chain length scales primarily dictated by the presence of anchoring points on the GO substrate upon intercalation.

Region V: the low-energy bands at 74 cm^{-1} (VI) and 115 cm^{-1} (VII) arise from either torsional COC or CO internal rotations in nPEO. These features are considerably broader in the confined phase and closely resemble the vibrational density of states of a disordered amorphous polymer [25].

3.2. Host effects

The previous section has shown that the extreme two-dimensional confinement of EG and nPEO in GO at subnanometer length scales induces profound changes to the structure and dynamics of the polymer phase. In the present section, we address the question as to whether polymer-substrate interactions or purely geometric restrictions are the driving force governing this behaviour. To this end, we prepared and investigated a series of 2135PEO/GO intercalates with a variable degree of GO oxidation, as well as a specimen consisting of 2135PEO adsorbed on thermally reduced G sheets. The amount of intercalated PEO in GO varies from 9 to 27 wt% as the degree of oxidation is increased from an oxygen-to-carbon atomic ratio (O/C) of 0.29 to 0.39 [13]. From this point onwards, the amount of intercalated PEO undergoes a slight decrease to 23 wt% at 0.40 O/C. The INS and DSC data of these materials are quite insensitive to the degree of oxidation of the underlying GO host. In contrast, these data show significant differences in the behaviour of the adsorbed 2135PEO phase on G (PEO/G) compared to the intercalated 2135PEO phase [9]. The amount of PEO adsorbed on G increases to 28 wt% in spite of the low O/C of G (0.13), a result which can be explained in terms of the high (open) surface area characteristic of this material (BET area ca. $630 \text{ cm}^2/\text{g}$). Moreover, the DSC data for 2135PEO exhibits a clear glass transition (T_g) at 209 K and melting (T_m) at 304 K, noticeably lower than those of the bulk material (218 and 333 K, respectively). The INS data show clear differences in the spectrum of 2135PEO/G compared to that of 2135PEO/GO (see reference [9]). In particular, the CH_2 rocking band at 815 cm^{-1} in 2135PEO/GO shifts to 835 cm^{-1} , an intermediate energy between that of the confined and the crystalline 2135PEO

phase (846 cm^{-1}). This spectral shift indicates a sensible increase in the population of gauche conformers in 2135PEO/G compared to that in 2135PEO/GO. Table 2 summarises the CH_2 rocking-band positions for bulk-crystalline and confined specimens in GO and G. These findings are consistent with our DSC experiments showing clear signs of crystal melting in PEO/G. From the present comparison between GO- and G-based materials, we conclude that the geometry of the host medium plays a critical role at dictating the ultimate properties of the confined polymer phase, particularly under conditions of extreme (subnanometer) spatial confinement.

Table 2. INS bands (in cm^{-1}) corresponding to the CH_2 rocking vibrations of methylene groups in 2135PEO in the bulk crystal, intercalated in GO, and adsorbed onto G sheets.

phase	peak 1	peak 2	conformation
crystalline	946	845	<i>tgt</i>
adsorbed on G	930	835	intermediate
intercalated in GO	914	815	<i>ttt</i>

4. Perspectives

High-resolution neutron spectroscopy provides access to structural and dynamical information on confined hydrogenous materials not accessible by any other experimental probe. As the present work highlights, basic prerequisites include access to a broad range of energy transfers ($0\text{-}4000\text{ cm}^{-1}$) as well as tight resolution (1-2 %) across the entire spectral range. The former is of particular relevance to assess the effects of spatial confinement on both intra and intermolecular modes, whereas the latter is of paramount importance in order to follow subtle yet at the same time significant changes to macromolecular conformation in the fingerprint region of the vibrational spectrum below 1500 cm^{-1} . At the present time, the TOSCA spectrometer at the ISIS Facility provides these unique capabilities on a routine basis, yet we note that both LAGRANGE at the ILL (France) and VISION at the SNS (USA) are now in a position to tackle these challenges with success as well. The present INS measurements have been restricted to low temperatures as our primary objective was to probe the VDOS of the confined hydrogenous phase. Notwithstanding the above, extension of these high-resolution INS studies to higher temperatures also offers the exciting prospects of studying the emergence of critical phenomena such as two-dimensional melting in these complex materials. Such a task is significantly more intricate than previous studies of atomic and molecular intercalation in pristine graphite [26, 27, 28, 29], and might well require a judicious combination of both inverted- and direct-geometry INS instrumentation in order to cover a sufficiently broad spectral range with adequate resolution.

To conclude, we note that further work is also underway to validate detailed computational models of extreme molecular and macromolecular confinement in well-defined nanostructured materials using INS, as well as to link polymer conformation and vibrational structure with the dynamical response and transport properties of these novel materials at longer time scales, accessible via quasielastic neutron scattering techniques and dielectric spectroscopy.

Acknowledgements

The authors gratefully acknowledge the continued support from the Spanish Ministry of Education (MAT2007-63681), Basque Government (IT-436-07), Gipuzkoako Foru Aldundia

(2011-CIEN-000085-01), and the UK Science and Technology Facilities Council. F.B.-B. acknowledges financial support from BERC-MPC.

References

- [1] Painter P C, Coleman M and Koenig J 1982 *The Theory of Vibrational Spectroscopy and its Application to Polymeric Materials* (New York: John Wiley & Sons)
- [2] Aranda P and Ruiz-Hitzky E 1992 *Chem. Mater.* **4** 1395–1403
- [3] Matsuo Y, Tahara K and Sugie Y 1997 *Carbon* **35** 113–120
- [4] Miwa Y, Drews A R and Schlick S 2008 *Macromolecules* **41** 4701–4708
- [5] Nemanich R, Lucovsky G and Solin S 1977 *Solid State Commun.* **23** 117–120
- [6] Ferrari A C 2007 *Solid State Commun.* **143** 47–57
- [7] Reich S and Thomsen C 2004 *Philos. Trans. Roy. Soc. London. Ser. A Math. Phys. Eng. Sci.* **362** 2271–2288
- [8] Colognesi D, Celli M, Cilloco F, Newport R J, Parker S F, Rossi-Albertini V, Sacchetti F, Tomkinson J and Zoppi M 2002 *Appl. Phys. A-Mater. Sci. Process.* **74** s64
- [9] Barroso-Bujans F, Fernandez-Alonso F, Pomposo J A, Cerveny S, Alegria A and Colmenero J 2012 *ACS Macro Lett.* **1** 550–554
- [10] Barroso-Bujans F, Fernandez-Alonso F, Cerveny S, Arrese-Igor S, Alegria A and Colmenero J 2012 *Macromolecules* **45** 3137–3144
- [11] Barroso-Bujans F, Fernandez-Alonso F, Cerveny S, Parker S F, Alegria A and Colmenero J 2011 *Soft Matter* **7**(16) 7173–7176
- [12] Brodie B C 1859 *Philos. Trans. Roy. Soc. London* **149** 249–259
- [13] Barroso-Bujans F, Fernandez-Alonso F, Pomposo J A, Enciso E, G Fierro J L and Colmenero J 2012 *Carbon* **50** 5232–5241
- [14] Barroso-Bujans F, Alegria A, Pomposo J A and Colmenero J 2013 *Macromolecules* **46** 1890–1898
- [15] Cerveny S, Barroso-Bujans F, Alegria A and Colmenero J 2010 *J. Phys. Chem. C* **114** 2604–2612
- [16] Yoshihara T, Tadokoro H and Murahashi S 1964 *J. Chem. Phys.* **41** 2902–2911
- [17] Matsuura H and Miyazawa T 1969 *J. Polym. Sci., Part A2: Polym. Phys.* **7** 1735–1744
- [18] Maxfield J and Shepherd I W 1975 *Polymer* **16** 505–509
- [19] Yang X, Su Z, Wu D, Hsu S L and Stidham H D 1997 *Macromolecules* **30** 3796–3802
- [20] Papke B L, Ratner M A and Shriver D F 1981 *J. Phys. Chem. Solids* **42** 493–500
- [21] Koenig J L and Angood A C 1970 *J. Polym. Sci., Part A2: Polym. Phys.* **8** 1787–1796
- [22] Matsuura H and Miyazawa T 1967 *Bull. Chem. Soc. Jpn.* **40** 85–94
- [23] Matsuura H, Hiraiishi M and Miyazawa T 1972 *Spectrochim. Acta, Part A* **28** 2299–2304
- [24] Luo R S and Jonas J 2001 *J. Raman Spectrosc.* **32** 975–978
- [25] Frick B and Fetters L J 1994 *Macromolecules* **27** 974–980
- [26] Enoki T, Endo M and Suzuki M 2003 *Graphite intercalation compounds and applications* (Oxford University Press, Incorporated)
- [27] Simon C, Rosenman I, Batallan F, Lartigue C and Legrand J F 1992 *Phys. Rev. B* **45**(6) 2694–2698
- [28] Simon C, Rosenman I, Batallan F, Rogerie J, Legrand J F, Magerl A, Lartigue C and Fuzellier H 1990 *Phys. Rev. B* **41**(4) 2390–2397
- [29] Simon C, Rosenman I, Batallan F, Pepy G and Lauter H 1988 *Synth. Met.* **23** 147–153